

Melatonin prevents cisplatin- and staurosporine-induced apoptosis in skeletal muscle cells *in vitro*

Valentina Baldassarri, Barbara Canonico, Sabrina Burattini, Michela Battistelli, Stefano Papa, Elisabetta Falcieri, Sara Salucci

Department of Biomolecular Sciences, University of Urbino Carlo Bo, Urbino, Italy

Corresponding author: Sara Salucci, Department of Biomolecular Sciences, University of Urbino Carlo Bo, Via Ca' le Suore 2, 61029 Urbino, Italy.

Tel.: +39 0722 304248.

E-mail: sara.salucci@uniurb.it

Key words: Apoptotic triggers; melatonin; skeletal muscle death; oxidative stress; intrinsic pathway.

Acknowledgements: A special thank is due to dr A. Barocci for her skillful assistance in the English revision.

SUMMARY

Oxidative stress is one of the major players in initiating apoptotic cell death in skeletal muscle, contributing to mitochondria-mediated apoptotic signaling in several myopathies as well as in a variety of atrophic conditions. Melatonin, known as a free radical scavenger and able to stimulate anti-oxidant enzyme efficiency in different cell models, could provide protection against oxidative stress in skeletal muscle too. Here, melatonin effect has been investigated in C2C12 myoblasts, exposed to apoptotic chemical triggers which lead to radical oxygen species increase. Cells were treated with melatonin before exposure to cisplatin or staurosporine and cell behavior investigated by means of cytometric and morpho-functional analyses. In myoblasts, melatonin prevents mitochondria damage and apoptosis induced by cisplatin, and, to a lesser extent, by staurosporine, as appeared after ultrastructural observations. In particular, if compared to treatments alone, samples pre-treated with melatonin before chemicals showed preserved nuclei and organelles, a reduced *in situ* DNA fragmentation and a decrease of lipid peroxidation events. In conclusion, these findings evidence melatonin ability in preventing mitochondrial dysfunctions and, as a consequence, the activation of skeletal muscle apoptosis.

Received for publication: 6 February 2018. Revision received: 26 March 2018. Accepted for publication: 20 April 2018.

©Copyright V. Baldassarri *et al.*, 2018

Licensee PAGEPress, Italy

microscopie 2018; 29:7334

doi:10.4081/microscopie.2018.7334

This article is distributed under the terms of the Creative Commons Attribution Noncommercial License (by-nc 4.0) which permits any noncommercial use, distribution, and reproduction in any medium, provided the original author(s) and source are credited.

Introduction

Excessive reactive oxygen species (ROS) levels are key initiators and mediators of dysfunctions in a variety of cells. These include deep alterations in cell signaling, metabolism, transcriptional activity, mitochondrial function, and increased activation of apoptotic pathways (Allen and Tresini, 2000; Calvani *et al.*, 2013; SullivanGunn and Lewandowski, 2013; Bargiela *et al.*, 2015; Marzetti *et al.*, 2017).

Apoptosis is necessary for skeletal muscle homeostasis since it plays a key role in coordinating myoblast proliferation and muscle differentiation (Shiokawa *et al.*, 2002; Burattini *et al.*, 2016; Salucci *et al.*, 2016; Salucci *et al.*, 2017). On the other hand, its misregulation impairs skeletal muscle functions and it is associated with several muscle diseases (Loro *et al.*, 2010; Merlini *et al.*, 2008; Davis *et al.*, 2013; Cea *et al.*, 2016; McClung *et al.*, 2017; Fan *et al.*, 2017; Fontes-Oliveira *et al.*, 2017)

Melatonin, or N-acetyl-5-methoxytryptamine, the pineal hormone exhibits strong anti-oxidant effects against a variety of ROS, by stimulating the production of anti-oxidant enzymes too. In literature we can find evidence indicating that melatonin leads to clinical improvement of certain muscle pathological conditions, by acting as an antioxidant molecule (Chen *et al.*, 2009; Hibaoui *et al.*, 2009; Chahbouni *et al.*, 2010).

Furthermore, our previous works demonstrated melatonin capability in preventing apoptosis induced by chemical agents in U937 cells (Salucci *et al.*, 2010, 2014).

The aim of this work was to test melatonin effects on the cytotoxicity induced by chemical triggers in C2C12 myoblasts, thereby verifying its ability to prevent apoptosis. The chemicals, chosen for their multiple mechanisms of action all involving, at least in part, the induction of oxidative stress, are:

cisplatin, which reacts *in vivo* by binding to and causing intra-strand crosslinking of DNA (Todd and Lippard, 2009), triggering apoptosis *via* p21-p53 proteins or directly through the Bcl-2-associated X protein (Bax)

staurosporine, a Protein kinase C (PKC) inhibitor which induces an early mitochondrial membrane potential ($\Delta\Psi_m$) loss, which in turn stimulates MOMP and the cytochrome c release (Charlot *et al.*, 2004) and which is also able to directly activate caspase-3

First of all, we carried on some cytometric analyses, used to better characterize cell death as a result of the chemical treatments.

Then, the cellular response to melatonin and treatments was investigated at the morpho-functional level by means of ultrastructural analysis. Moreover, DNA fragmentation and

membrane integrity were evaluated, at confocal laser scanning microscopy, by means of TUNEL technique and 10-nonyl acridine orange staining respectively.

Materials and Methods

Cell culture and treatments

C2C12 adherent myoblasts (cultured in flask for electron microscopy and flow cytometry analyses, or in multi-well dishes for confocal microscopy analyses) were grown in DMEM supplemented with 10% fetal bovine serum (FBS) in the presence of 100 $\mu\text{g/ml}$ penicillin/streptomycin and 1% L-glutamine (Salucci *et al.*, 2013).

Cells were monitored using a Nikon Eclipse TE 2000-S IM equipped with a DN 100 Nikon digital camera system. On the basis of our previous works (Salucci *et al.*, 2013; Battistelli *et al.*, 2014), we established that the best treatments for apoptosis induction in our cell line were:

- 30 μM cisplatin, for 24 h
- 0.25 μM staurosporine, for 24 h

In addition, samples were pre-incubated with 100 μM melatonin, 24 h before apoptosis induction. For each technique, control sample and 24 h-melatonin treatment were also analyzed. Melatonin (Sigma, St Louis, MO, USA) was first dissolved in absolute ethanol at the initial concentration of 100 mM, and then diluted at the final 100 μM concentration in culture medium (Salucci *et al.*, 2016).

Flow cytometry (FC)

Samples were analyzed as ethanol fixed cells to evaluate DNA content, using propidium iodide (PI) labeling, or as fresh cells for other investigations.

For cell cycle profile, cells were centrifuged and fixed with 70% cold ethanol and pellets were kept at -20°C for at least 1 day. Then, pellets were washed twice in PBS and re-suspended in a citrate buffer containing 20 $\mu\text{g/ml}$ PI and 100 $\mu\text{g/ml}$ RNase A. Cells were additionally treated with 0.2% Triton X-100 and re-suspended 2-3 times using small pipette tips to increase cellular disaggregation.

To label fresh cells, we added each fluorochrome in the appropriate volume to cell suspension. The cardiolipin-sensitive probe 10-nonyl acridine orange (NAO) was used to monitor mitochondrial lipid changes (Canonica *et al.*, 2016); cells were incubated with 100 nM NAO, for 20 min at 37°C .

The fluorescent probe 5-(and 6-)-chloromethyl-2',7'-dichlorodihydrofluorescein diacetate, acetyl ester (CM-H2DCFDA) (Molecular Probes, OR), useful as indicator of ROS, was solubilized in dimethyl sulfoxide (DMSO; Sigma) and then diluted to a final concentration of 10 μM in PBS cellular pellets and incubated in this buffer (200 μl) for 30

min at 37°C. Then cells were washed once with PBS and were analyzed by FC, by registering at least 10.000 events for each different sample. Fixed and fresh samples were kept at 37°C in the dark for at least 30 min and analyzed by means of a FACScalibur flow cytometer equipped with two lasers (Canonico *et al.*, 2010; NAO excitation 495 nm; NAO emission 520 nm; CM-H2DCFDA excitation 488 nm; CM-H2DCFDA emission 530 nm). Data were analyzed using CellQuest™ flow cytometry software (Becton Dickinson, San Jose, CA).

In addition, each sample has been treated for 2 h with caspase-9 inhibitor (Ac-LEHD-CMK, Calbiochem, Billerica, MS, USA) before apoptosis induction and then processed for NAO and CM-H2DCFDA staining.

Transmission electron microscopy (TEM)

Cells, grown in flasks, were rinsed in 0.15 M phosphate buffer (pH 7.4), fixed *in situ* with 2.5% glutaraldehyde for 40 min, and then gently scraped, centrifuged and post-fixed in 1% OsO₄ for 1 h. Pellets were dehydrated, using increasing concentrations of ethanol, and embedded in araldite.

Ultrathin sections were stained with uranyl acetate and lead citrate and then analyzed using a Philips CM10 electron microscope (Burattini *et al.*, 2013).

Confocal laser scanning microscopy (CLSM)

For CLSM analysis, immunofluorescence (IF) techniques were carried out on coverslips. Samples were rinsed with 0.1M PBS pH 7.4 and fixed *in situ* with 4% paraformaldehyde in PBS, for 30 min at room temperature (R.T.). For the TUNEL technique, after a further washing with PBS, samples were permeabilized with a 2:1 mixture of ethanol and acetic acid, for 5 min at -20°C. Procedures were carried out according to the manufacturer's instructions and all reagents were part of the Apoptag Plus kit (D.B.A.). Briefly, cells were treated with the terminal deoxynucleotidyl transferase (TdT) buffer for 10 min at R.T. and incubated with the reaction buffer containing the TdT enzyme for 1 h, at 37°C in a humidified chamber (Burattini *et al.*, 2016). The reaction was blocked using the stop buffer for 10 min. Cells were incubated with a FITC-conjugated anti-digoxigenin antibody for 30 min at R.T. For mitochondrial analysis, 50 nM NAO for 10 min was used.

Slides were finally mounted with an anti-fading medium (Vectashield, Vector Labs). Images were collected with a Leica TCS-SP5 Confocal connected to a DMI 6000 CS Inverted Microscope (Leica Microsystems CMS GmbH) and analyzed using the Leica Application Suite Advanced Fluorescence (LAS AF) software. Samples were examined using oil immersion objective lenses (40x N.A. 1.25; 63x N.A. 1.40). Excitation was at 488 nm (FITC and NAO);

emission signals were detected at 519 nm (NAO) or 525 nm (FITC). CLSM images are presented as single-plane images or Z-stack projections.

For each treatment, two hundred cells were counted to quantify myoblasts with TUNEL positive nuclei. The percentage of stained nuclei was reported in a graphic as mean \pm standard deviation.

Statistical analysis

All data are presented as mean \pm standard deviation. Student's *t*-test has been applied to compare the results. A value of $P < 0.05$ has been considered as significant threshold.

Results

Flow cytometry

Cell cycle analysis

PI staining intensity reflects DNA content for each cell and plotting permits to obtain a DNA histogram pattern when we obtained the data table (Figure 1). Generally, in 'classic' apoptotic models, the evidence of a clear sub-G1 peak reveals the presence of an apoptotic cell population. Nevertheless, in C2C12 myoblasts this hypodiploid peak is not always observed and the DNA content distribution appears more peculiar (see cytogram in Figure 1). In our experiments, treatments induce a significant DNA cleavage, absent in the control condition. In particular, cisplatin exposure shows the clearest sub-G1 peak.

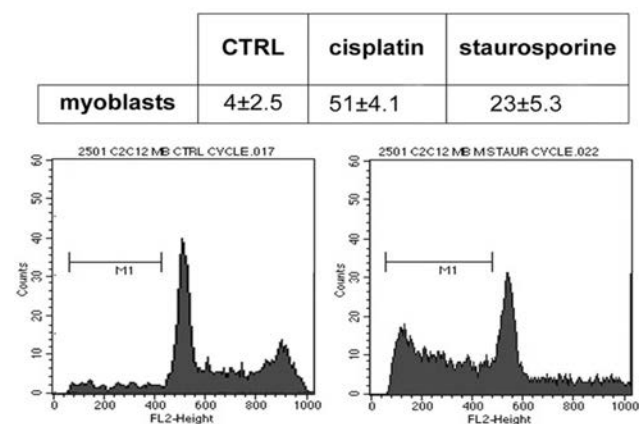


Figure 1. Data table showing percentage of sub-G1 events in each experimental condition. Data are from 3 independent experiments and are furnished as mean \pm SD. Student's *t*-test reveals that all treated samples show a highly significant ($p < 0.01$) increase in sub-G1 events, compared to control condition. An example of PI-DNA cytogram of control and staurosporine-treated cells, can be observed.

NAO detection

The appearance of cells with low NAO fluorescence intensity (dim events) indicates cardiolipin oxidation inside the mitochondria. In fact, cardiolipin undergoes peroxide oxidation by cytochrome *c* in the presence of hydrogen peroxide or other chemicals, and oxidized cardiolipin has a low affinity for NAO. Furthermore, in literature we can find several reports demonstrating that cardiolipin oxidation is related to the apoptotic process (Kagan *et al.*, 2005; Ott *et al.*, 2007); then NAO staining not only provides indication on the structural integrity of the mitochondria but also on the cell condition and, in particular, on the activation of the intrinsic apoptotic pathway.

Frequencies of events characterized by normal cardiolipin (bright event percentage) decreased after cisplatin and staurosporine (Figure 2), evidencing that the chemicals used are able to trigger a mitochondrial impairment. In concomitance with each treatment a caspase-9 inhibitor (iCasp-9) was also used and we observed that its administration increases, in cisplatin treated samples, the myoblast percentage with non-oxidized cardiolipin, demonstrating, at least in part, that the intrinsic apoptotic pathway is involved in initiating cell death. A different behavior appeared when iCasp-9 was added to staurosporine treated samples with an evident increase of oxidized cardiolipin.

Taking into account the mean fluorescence intensity (MFI) values for NAO labeling, an intense peroxidation at the single cell level can be identified for cisplatin and stau-

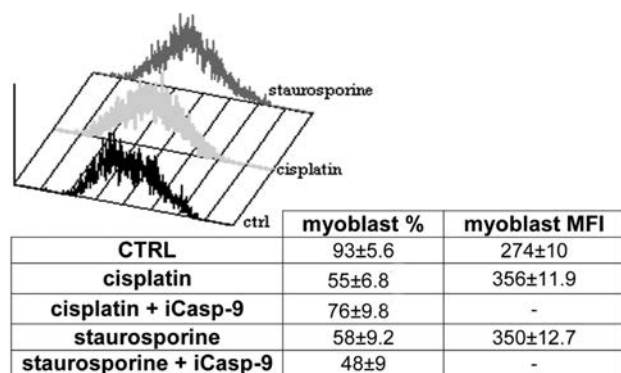


Figure 2. Data table indicating the % of NAO bright events and NAO MFI values. An example of NAO cytochrome c fluorescence histogram can be observed for each treatment. Data are from 3 independent experiments and are furnished as mean±SD. Student's *t*-test shows that bright event decrease is significant ($p < 0.01$) in cisplatin and staurosporine samples, compared to control condition. After iCasp-9 administration in cisplatin-treated sample the increase of bright events resulted to be significant ($p < 0.05$), compared to cisplatin alone.

rosporine. This is in accordance with the fact that the MFI value may transiently rise when the level of ROS is high even if mitochondria are not yet degenerated (Apostolova *et al.*, 2010).

CM-H₂CFDA analysis

We observe that chemical treatments induce a significant ROS increase compared to control, as showed by the increase in the percentage of brightly-fluorescing events after CM-H₂CFDA staining (Figure 3). However, in the case of staurosporine the number of dim events was larger compared to the bright events (*data not shown*), indicating that oxidative stress induction is not the main mechanism of action of this chemical. iCasp-9 administration, as expected, further increases ROS production in the samples treated with cisplatin. Conversely, in concomitance with staurosporine, iCasp-9 causes a bright event decrease.

Electron microscopy and CLSM

Ultrastructural observations showed control myoblasts, tightly adherent to the substrate, with a fusiform shape

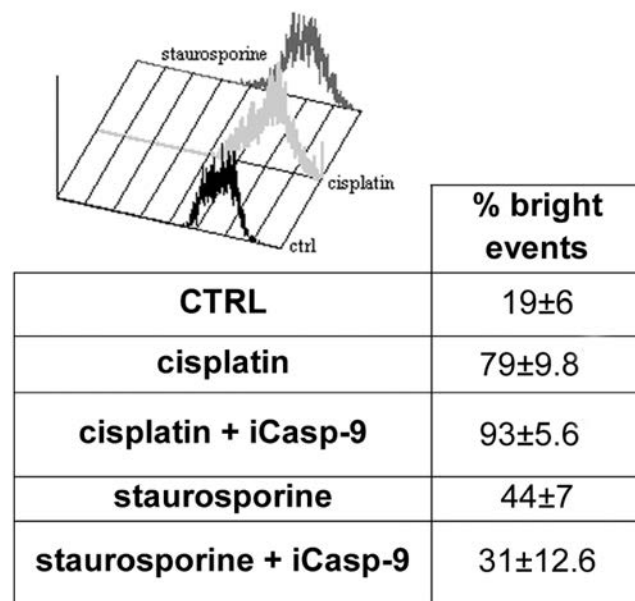


Figure 3. Data table showing % of CM-H₂CFDA bright events. An example of CM-H₂CFDA fluorescence histogram can be observed for each treatment. Data are from 3 independent experiments and are furnished as mean±SD. Student's *t*-test shows that the increase in bright events is highly significant ($p < 0.01$) in cisplatin, compared to control condition, and it is statistically significant ($p < 0.05$) in staurosporine samples. Also after iCasp-9 administration in cisplatin-treated sample the increase of bright events resulted to be statistically significant ($p < 0.05$), compared to cisplatin alone.

(Figure 4A); the cytoplasm and organelles were well preserved and showed a central nucleus with diffuse chromatin and nucleoli (Figure 4A). The TUNEL technique did not reveal any nuclear labeling (Figure 5A); NAO fluorescence was very intense, thanks to the presence of preserved mitochondria (Figure 5B). Myoblasts, exposed to 100 μ M melatonin, did not reveal any changes compared to the control condition (Figure 4B); melatonin did not affect the nuclear behavior (Figure 5C) nor the mitochondria activity (Figure 5D).

After cisplatin exposure, cytoplasmic vacuolization, chromatin condensation and nuclear pore translocation occurred, and sometimes apoptotic bodies were observed (Figure 4C-D). A large number of TUNEL positive nuclei (Figure 5E) was detected; moreover, mitochondria membrane integrity has been lost, as evidenced by NAO fluorescence reduction (Figure 5F). In samples pre-treated with melatonin before cisplatin exposure, myoblasts appeared normal and chromatin was not condensed (Figure 5E). No DNA fragmentation was observed (Figure 5G) and NAO fluorescence was comparable to the control condition (Figure 5H).

After 24 h of staurosporine exposure, a diffuse cell dam-

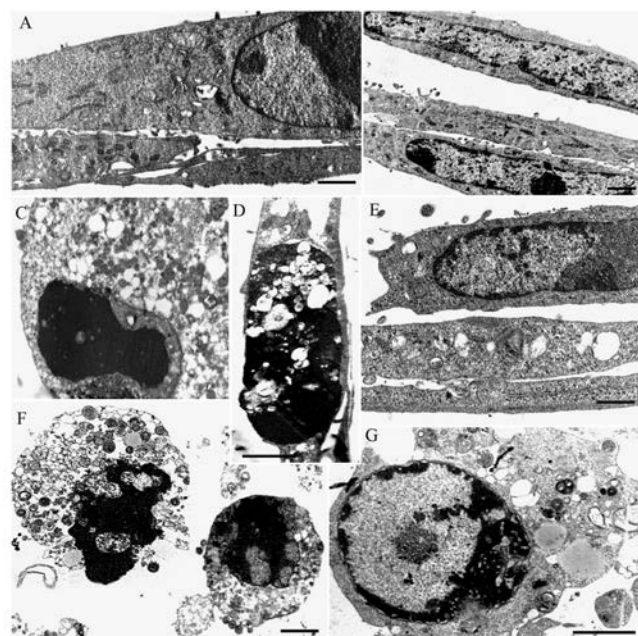


Figure 4. Ultrastructural observations show cells in control condition (A) and those pre-treated with melatonin (B). Samples exposed to CP (C, D) or ST (F), and those pre-treated with melatonin before exposure to CP (E) or ST (G) can be observed. Scale bars: A-E) 1 μ m; F,G) 2 μ m. (CP: cisplatin and ST: staurosporine).

age was observed on myoblasts; numerous apoptotic bodies, containing condensed chromatin, were visible and cells in secondary necrosis appeared (Figure 4F). Moreover, TUNEL is strongly positive (Figure 5I) and NAO labeling

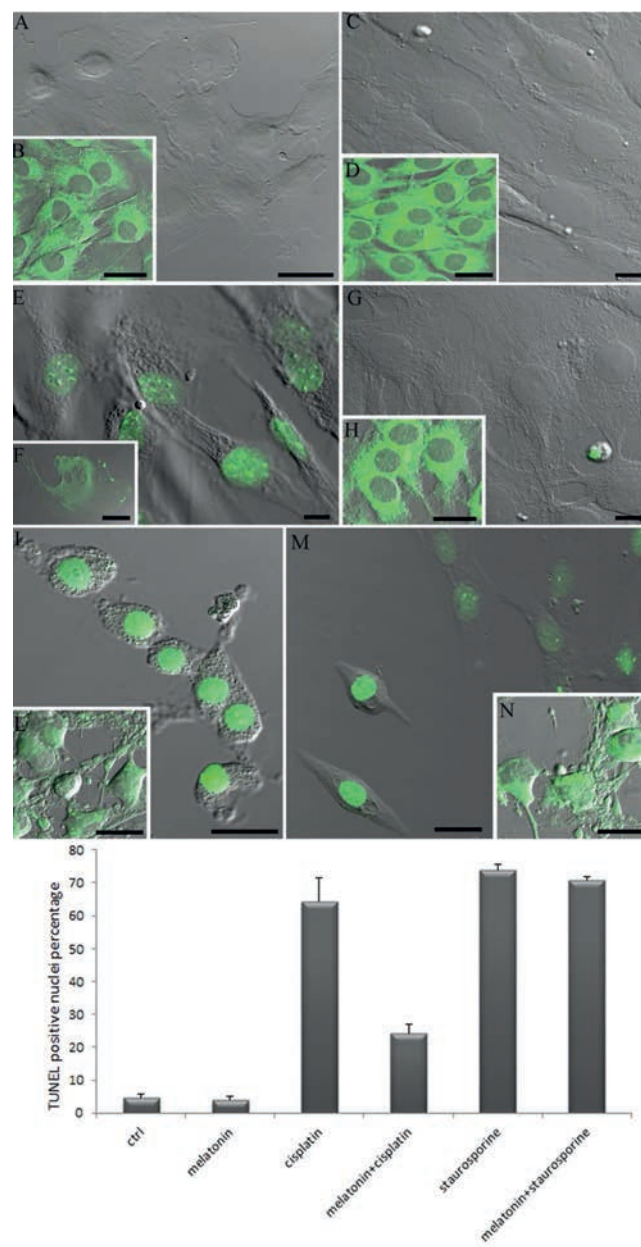


Figure 5. TUNEL (A, C, E, G, I, M) and NAO (B, D, F, H, L, N) reaction can be observed in control condition (A, B), after melatonin treatment (C, D), in cells exposed to CP (E, F) or ST (I, L) and in those pre-treated with melatonin and then exposed to CP (G, H) or ST (M, N). Scale bars: A,B,D,H,L,N) 10 μ m; I,M) 5 μ m; C, E-G) 2.5 μ m. The graphic represents the percentage of TUNEL-positive cells in the different experimental conditions.

shows a weak fluorescence (Figure 5L). Melatonin pre-treatment seems to delay staurosporine effect. Myoblasts, even if in the presence of nuclear damage, retained their shape and maintained the plasma membrane integrity (Figure 4G). At CLSM, TUNEL positivity decreased, with an improvement of the cell morphology (Figure 5M); in fact, some myoblasts appeared rounded, but most of them were still adherent with an elongated shape. NAO fluorescence intensity seemed slightly increased compared to treatment alone (Figure 5N).

The graphic in Figure 5 describes the nuclear behavior of control and treated cells after TUNEL reaction. A conspicuous number of TUNEL positive nuclei appeared after cisplatin and staurosporine administration compared to the control condition. According to the ultrastructural observations, the ability of melatonin to reduce *in situ* DNA fragmentation is evident in samples exposed to cisplatin.

Discussion

This work describes the effects of two of the most well-known chemicals and the action of melatonin against these apoptotic triggers on *in vitro* C2C12 myoblasts.

In particular, these findings demonstrate that melatonin is able to prevent the damage and/or cell death induced by cisplatin. The analyses of cardiolipin peroxidation and the results of caspase-9 inhibition have shown that cisplatin induces apoptosis primarily *via* the mitochondrial pathway. Moreover, the fact that melatonin prevents the death induced by this trigger indicates that this compound acts by affecting the mitochondrial pathway. Melatonin pre-treatment before cisplatin exposure leads to an improvement of the cell viability, preventing nuclear fragmentation and improving mitochondrial integrity and function.

Staurosporine action is not completely inhibited by melatonin but only delayed, probably due to the fact that its mechanism of action provides only a subordinate role for the mitochondrial pathway. Staurosporine induces apoptosis involving different apoptotic pathways which include both its ability to act as a non-selective inhibitor of a diverse array of different kinases and its ability to induce mitochondrial caspase activation (Stepczynska *et al.*, 2001). Our experiments, supported by flow cytometry analyses, show that probably the main mechanism of staurosporine action does not pass through the ROS cascade.

In conclusion, this morpho-functional study emphasizes the potential role of melatonin as modulators of oxidative stress and apoptotic cell death in skeletal muscle cells.

References

- Apostolova N, Gomez-Sucerquia LJ, Moran A, Alvarez A, Blas-Garcia A, Esplugues JV. Enhanced oxidative stress and increased mitochondrial mass during efavirenz-induced apoptosis in human hepatic cells. *Br J Pharmacol* 2010;160:2069-84.
- Bargiela A, Cerro-Herreros E, Fernandez-Costa JM, Vilchez JJ, Llamusi B, Artero R. Increased autophagy and apoptosis contribute to muscle atrophy in a myotonic dystrophy type 1 Drosophila model. *Dis Model Mech* 2015;8:679-90.
- Battistelli M, Salucci S, Burattini S, Falcieri E. Further considerations on *in vitro* skeletal muscle cell death. *Muscles Ligaments Tendons J* 2014;3:267-74.
- Burattini S, Battistelli M, Codenotti S, Falcieri E, Fanzani A, Salucci S. Melatonin action in tumor skeletal muscle cells: an ultrastructural study. *Acta Histochem* 2016;118:278-85.
- Burattini S, Salucci S, Baldassarri V, Accorsi A, Piatti E, Madrona A, et al. Anti-apoptotic activity of hydroxytyrosol and hydroxytyrosyl laurate. *Food Chem Toxicol* 2013;55:248-56.
- Calvani R, Joseph AM, Adihetty PJ, Miccheli A, Bossola M, Leeuwenburgh C, et al. Mitochondrial pathways in sarcopenia of aging and disuse muscle atrophy. *Biol Chem* 2013;394:393-414.
- Canonica B, Betti M, Luchetti F, Battistelli M, Falcieri E, Ferri P, et al. Flow cytometric profiles, biomolecular and morphological aspects of transfixed leukocytes and red cells. *Cytometry B Clin Cytom* 2010;78:267-78.
- Canonica B, Cesarini E, Salucci S, Luchetti F, Falcieri E, Di Sario G, et al. defective autophagy, mitochondrial clearance and lipophagy in Niemann-Pick Type B lymphocytes. *PLoS One* 2016;11:e0165780.
- Cea LA, Puebla C, Cisterna BA, Escamilla R, Vargas AA, Frank M, et al. Fast skeletal myofibers of mdx mouse, model of Duchenne muscular dystrophy, express connexin hemichannels that lead to apoptosis. *Cell Mol Life Sci* 2016;73:2583-99.
- Chahbouni M, Escames G, Venegas C, Sevilla B, García JA, López LC, et al. Melatonin treatment normalizes plasma pro-inflammatory cytokines and nitrosative/oxidative stress in patients suffering from Duchenne muscular dystrophy. *J Pineal Res* 2010;48:282-9.
- Charlot JF, Prétet JL, Haughey C, Mouglin C. Mitochondrial translocation of p53 and mitochondrial membrane potential ($\Delta\Psi_m$) dissipation are early events in staurosporine-induced apoptosis of wild type and mutated p53 epithelial cells. *Apoptosis* 2004;9:333-43.
- Chen Z, Chua CC, Gao J, Chua KW, Ho YS, Hamdy RC, et

- al. Prevention of ischemia/reperfusion-induced cardiac apoptosis and injury by melatonin is independent of glutathione peroxidase 1. *J Pineal Res* 2009;46:235-41.
- Davis J, Kwong JQ, Kitsis RN, Molkentin JD. Apoptosis repressor with a CARD domain (ARC) restrains Bax-mediated pathogenesis in dystrophic skeletal muscle. *PLoS One* 2013;8:e8205.
- Fan J, Yang X, Li J, Shu Z, Dai J, Liu X, et al. Spermidine coupled with exercise rescues skeletal muscle atrophy from D-gal-induced aging rats through enhanced autophagy and reduced apoptosis via AMPK-FOXO3a signal pathway. *Oncotarget* 2017;8:17475-90.
- Fontes-Oliveira CC, Steinz M, Schneiderat P, Mulder H, Durbeej M. Bioenergetic impairment in congenital muscular dystrophy type 1A and Leigh Syndrome muscle cells. *Sci Rep* 2017;7:45272.
- Hibaoui Y, Roulet E, Ruegg UT. Melatonin prevents oxidative stress-mediated mitochondrial permeability transition and death in skeletal muscle cells. *J Pineal Res* 2009;47:238-52.
- Kagan VE, Tyurin VA, Jiang J, Tyurina YY, Ritov VB, Amoscato AA, et al. Cytochrome c acts as a cardiolipin oxygenase required for release of proapoptotic factors. *Nat Chem Biol* 2005;1:223-32.
- Loro E, Rinaldi F, Malena A, Masiero E, Novelli G, Angelini C, et al. Normal myogenesis and increased apoptosis in myotonic dystrophy type-1 muscle cells. *Cell Death Differ* 2010;17:1315-24.
- Luchetti F, Canonico B, Curci R, Battistelli M, Mannello F, Papa S, et al. Melatonin prevents apoptosis induced by UV-B treatment in U937 cell line. *J Pineal Res* 2006;40:158-67.
- Marzetti E, Calvani R, Tosato M, Cesari M, Di Bari M, Cherubini A, et al. Sarcopenia: an overview. *Aging Clin Exp Res* 2017;29:11-7.
- McClung JM, McCord TJ, Ryan TE, Schmidt CA, Green TD, Southerland KW, et al. BAG3 (Bcl-2-associated athanogene-3) coding variant in mice determines susceptibility to ischemic limb muscle myopathy by directing autophagy. *Circulation* 2017;136:281-96.
- Merlini L, Angelin A, Tiepolo T, Braghetta P, Sabatelli P, Zamparelli A et al. Cyclosporin A corrects mitochondrial dysfunction and muscle apoptosis in patients with collagen VI myopathies. *Proc Natl Acad Sci USA* 2008;105:5225-9.
- Ott M, Zhivotovsky B, Orrenius S. Role of cardiolipin in cytochrome c release from mitochondria. *Cell Death Differ* 2007;14:1243-7.
- Prabhakaran K, Li L, Borowitz JL, Isom GE. Caspase inhibition switches the mode of cell death induced by cyanide by enhancing reactive oxygen species generation and PARP-1 activation. *Toxicol Appl Pharmacol* 2004;195:194-202.
- Reiter RJ, Tan DX, Manchester LC, Pilar Terron M, Flores LJ, Koppisepe S. Medical implications of melatonin: receptor-mediated and receptor-independent actions. *Adv Med Sci* 2007;52:11-28.
- Rodriguez MC and Tarnopolsky MA. Patients with dystrophinopathy show evidence of increased oxidative stress. *Free Radic Biol Med* 2003;34:1217-20.
- Salucci S, Baldassarri V, Canonico B, Burattini S, Battistelli M, Guescini M, et al. Melatonin behavior in restoring chemical damaged C2C12 myoblasts. *Microsc Res Tech* 2016;79:532-40.
- Salucci S, Battistelli M, Baldassarri V, Burini D, Falcieri E, Burattini S. Melatonin prevents mitochondrial dysfunctions and death in differentiated skeletal muscle cells. *Microsc Res Tech* 2017;80:1174-81.
- Salucci S, Burattini S, Baldassarri V, Battistelli M, Canonico B, Valmori A et al. The peculiar apoptotic behavior of skeletal muscle cells. *Histol Histopathol* 2013;28:1073-87.
- Salucci S, Burattini S, Battistelli M, Baldassarri V, Curzi D, Valmori A, et al. Melatonin prevents chemical-induced haemopoietic cell death. *Int J Mol Sci* 2014; 15:6625-40.
- Salucci S, Burattini S, Battistelli M, Chiarini F, Martelli AM, Sestili P, et al. Melatonin prevents hydrogen peroxide-induced apoptotic cell death. *Microscopie* 2010;13:51-7.
- Shiokawa D, Kobayashi T, Tanuma S. Involvement of DNase gamma in apoptosis associated with myogenic differentiation of C2C12 cells. *J Biochem Chem* 2002; 277:31031-7.
- Stepczynska A, Lauber K, Engels IH, Janssen O, Kabelitz D, Wesselborg S, et al. Staurosporine and conventional anticancer drugs induce overlapping, yet distinct pathways of apoptosis and caspase activation. *Oncogene* 2001;20:1193-202.
- Todd RC and Lippard SJ. Inhibition of transcription by platinum antitumor compounds. *Metallomics* 2009;1:280-91.